Passive Oscillations of Two Tandem Flexible Filaments in a Flowing Soap Film

Lai-Bing Jia and Xie-Zhen Yin*

Department of Modern Mechanics, University of Science and Technology of China, Hefei, Anhui, China 230027

(Received 2 November 2007; published 5 June 2008)

The passive oscillations of flexible filaments in a flowing soap film were investigated to learn the serial interaction between them. When arranged in tandem, the downstream filament flaps at the same frequency as that of the upstream one, but with a larger amplitude, whereas the upstream one is almost unaffected compared to the single filament case. The data analysis shows the downstream filament indeed extracts energy from the vortex street and receives greater force than the upstream one or a single filament in a uniform flow.

DOI: 10.1103/PhysRevLett.100.228104 PACS numbers: 47.63.M−, 87.19.rs

A group of fish swimming in unison might be one of the most enjoyable scenes in an aquarium. The phenomenon of fish schooling has been extensively studied for many years [1–5]. Besides the social and sensory factors, the hydrodynamic mechanism is an essential factor which promotes schooling since the fish in a school, swimming in the wake of preceding rows, conserve their energy. Based on a two-dimensional fish school model in inviscid flow, Weirs first proposed that an optimal configuration would be a diamond formation array [2]. The empirical evidence, however, is conflicting about the structure of a hydrodynamically efficient school [3,4]. The interference of fish in a school can be simply divided into parallel and serial interactions for the side-by-side and tandem arrangements, respectively. Any formation of more fish can be viewed as a combination of the basic arrangements. Dong investigated numerically the flow characteristics over traveling wavy foils in side-by-side arrangement [6]. As for the serial interaction of tandem fish, only a few references can be found [7,8]. Essentially the serial interaction results from a fish swimming in the vortex street shedding from foregoing fish. Similar research includes a series of important experiments recently by Lauder and his collaborators [5,7–10]. Liao studied the locomotion of live trout in the wake of a D cylinder, revealing that the trout adopt a novel mode of locomotion to slalom smoothly through the Kármán vortex street shedding from a D cylinder [5]. The electromyography demonstrates reduced muscle activity and conserved energy in this locomotion compared to that in free swimming. Beal found even anesthetized trout may maintain motion in the vortex street behind the D cylinder, which shows qualitatively that a dead fish can extract energy from the vortex street to produce thrust [9].

Research on the swimming behavior of fish schools in riverine environments certainly deals with a very complicated problem. Establishing a reasonable physical model from multifarious phenomena is a key in the mechanism research of fish schooling. The problem of fish swimming involves coupling between a flexible body and an ambient fluid. Usually an undulating foil with traveling wavy wall or a rigid foil with pitching and heaving motions are used to simulate the fish swimming locomotion. In 2000, Zhang introduced a method using flexible filaments immersed in a flowing soap film to simulate the undulatory propulsion motions of a fish [11]. A soap film is a convenient platform to carry out two-dimensional hydrodynamic experiments [12–16]. It can clearly reveal the interactions between a deformable body and the fluid. The passive problem of flapping filaments in a flowing soap film can also tell us much about undulatory propulsion in general [17,18]. Jia conducted experiments on the coupling mode between two flexible filaments in a side-by-side arrangement in a flowing soap film [19]. The interaction of flapping filaments in tandem arrangement is also a significant question in flapping propulsion, yet is seldom studied.

The work described here is motivated by these existing studies. Two flexible filaments immersed in tandem in a flowing soap film are used as a simplified two-dimensional model to investigate the serial interaction between them. In this Letter, the experimental observation is described and the analysis of forces variation and energy fluctuation based on an Euler-Bernoulli beam model is given. The goal is to explain quantitatively the mechanism of energy extraction by a flexible body from the vortex street.

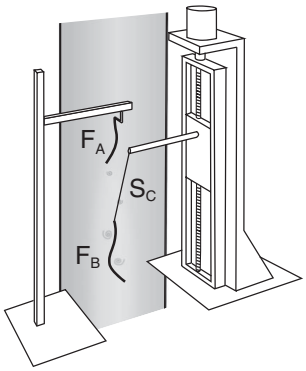

FIG. 1. Experimental schematic. The soap film flows downward. Two filaments (F_A and F_B) are immersed in the film. The silk fiber S_C is connected to the downstream filament at one end and to a linear stage outside of the soap film plane at the other end.

Our experiments on the tandem flapping filaments were conducted in a vertically flowing soap film tunnel [14,19]. The difficulty in studying the serial interaction of two filaments in a flowing soap film lies in preserving the vertical position of the downstream filament and, at the same time, allowing its leading edge to move freely in the wake shedding from the upstream one. Figure 1 shows our design for such an experiment. Two filaments (F_A and F_B) are immersed in tandem in a flowing soap film. The leading edge of F_A is fixed using a thin tube perpendicular to the film. The leading edge of F_B is fastened to a silk fiber (S_C). The trailing edges of both are free. S_C is connected to F_B at one end and to a linear stage outside of the film plane at the other end, where the stage position can be adjusted by a reduced speed motor. The diameter of F_A and F_B is 0.15 mm. S_C was pulled from a silkworm cocoon and its diameter is about 15 μm, of which the cross-sectional area is only 1/100 that of F_A and F_B. With the help of S_C, F_B can hold its position in the streamwise direction while keeping its leading edge free transversely. By adjusting the position of the stage, we can change the distance between the leading edges of F_A and F_B. The soap film is illuminated by three high pressure sodium lamps. Since the thickness of the soap film (about 1.5–3 μm, varying with flow speed) is only several times the lamp light wavelength (Na 589/590 nm), the interference between light reflected from two liquid-air interfaces of the soap film represents the thickness variation. These color fringes are passive scalars of the vorticity [15]. They are recorded by a high speed digital video camera (Mikrotron, MC1310) at 2004 frames/ s.

A single filament in a uniform flow starts flapping when the flow speed or the filament's length exceeds a critical value. A shear layer sheds from the filament's trailing edge and becomes unstable with successive small eddies along it. Concentrated vortices in the wake with opposite signs are alternately arranged forming a vortex street. Shorter filament length results in higher frequency and smaller amplitude. For example, at the uniform flow speed of 1.9 m/s, the frequencies for filaments of 20 and 40 mm length were measured to be 48.0 and 43.6 Hz with amplitudes 8.0 and 8.7 mm, respectively. However, the flow patterns of the vortex streets are similar [20]. The Strouhal numbers of both equal 0.2. Here the Strouhal number is defined as $\mathrm{St} = fA/U$, where f is the flapping frequency, A is the amplitude at the trailing edge of the filament, and U is the flow speed. This dimensionless number describes the oscillating flow mechanism. We tested different lengths of filaments and found the St number remains the same at a certain flow speed. In the following discussion, a 20 mm filament is used as F_A to produce a vortex street.

Figure 2 shows a typical interaction between two tandem filaments. The lengths of F_A and F_B (L_a and L_b) are both 20 mm. Figure 2(a) is a frame from the experiment video. F_B waved in the vortex street produced by F_A. By assembling the time sequenced vertical slices at the same horizontal position from the experiment video frames, we can get an image of the same position at different time. The result is similar to a photo taken by a streak camera. Figure 2(b) shows such an image produced by our video processing program. It represents the motion of the film and the filament at the position marked with ⊤ and ⊥ in Fig. 2(a), where rightward is the direction of time advance. The waving line at the center of the image is the trace of a small segment of F_B at different time. The segment is waving between vortices, as if it were pushed by the vortices, despite the pressure of vortex cores being actually lower than the surrounding fluid. The image indicates clearly that F_B slaloms smoothly between vortices. The phenomenon is similar to a fluid roller bearing, which is considered as a mechanism of drag reduction in the traveling wavy wall case [21]. Figure 2(c) describes how the whole F_B travels among vortex cores from right to left. Experiments show a lifeless filament can pass between the vortices rather than go through them, just like a trout swimming behind a D cylinder.

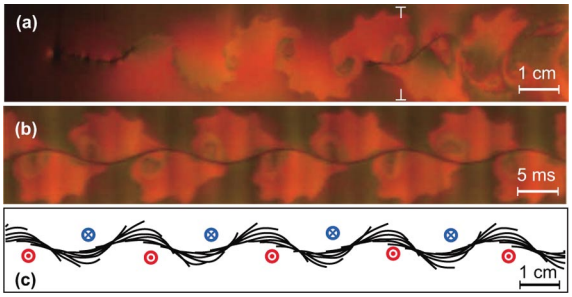

FIG. 2 (color). Interaction of two tandem filaments. (a) a frame in the experiment video ($L_a = L_b = 20$ mm, $U = 2.1$ m/s). The soap film is flowing from left to right. (b) is the combination of time sequenced vertical slices of video frames at the position marked with ⊤ and ⊥ in (a). (c) depicts how F_B slaloms between vortex cores.

A systematical study was carried out at low, medium and high soap film velocities. Two lengths of filament, 20 and 40 mm, were adopted as F_B. The distance (d) between the leading edges of F_A and F_B was varied systemically. Figure 3 shows the statistical results. At low flow speed, $U = 1.3$ and 1.5 m/s, the kinematic viscosity ν of the film was about 2×10^{-5} m^2/s and the Reynolds number Re based on the length of F_A was around 1400. At medium speed, $U = 1.9$ m/s, $\nu = 1.22 \times 10^{-5}$ m^2/s, and Re = 3000. And at high speed, $U = 2.1$ m/s, $\nu = 1.2 \times 10^{-5}$ m^2/s, and Re = 3500.

Figure 3(a) shows the relationship between the flapping frequency and the flow speed. In the experiments, F_B flapped at the same frequency as F_A in spite of its own frequency in a uniform flow. Figures 3(b)–3(d) give the statistical results of St vs d. At a certain flow speed, the St number of F_A changes little with different distance d. The St number stays around 0.2, which equals the value of a single filament in a uniform flow. In the experiments, F_A receives little influence from F_B and keeps its own pace

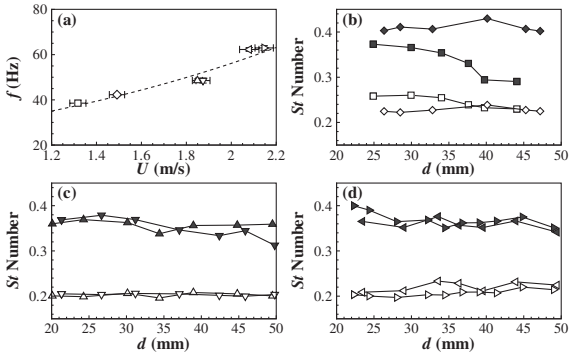

FIG. 3. Experimental results. -□- ($L_b = 20$ mm, $U = 1.3$ m/s), -◇- ($L_b = 40$ mm, $U = 1.5$ m/s), -△- ($L_b = 20$ mm, $U = 1.9$ m/s), -▽- ($L_b = 40$ mm, $U = 1.9$ m/s), -◁- ($L_b = 20$ mm, $U = 2.1$ m/s) and -▷- ($L_b = 40$ mm, $U = 2.1$ m/s). Symbols filled with white and gray denote F_A and F_B, respectively. (a) shows the flapping frequency f vs the flow speed U. Both F_A and F_B flap at the same frequency. (b),(c),(d) shows the St number of F_A and F_B vs d at low, medium, and high flow speed.

just like a single filament in a uniform flow. However, F_B in the flow wake is modulated by the shedding vortex. It flaps at the same frequency as F_A with larger amplitude, different from its flapping manner when placed alone in a uniform flow. This leads to a much larger St number than that of F_A or a single filament in a uniform flow. The value $\mathrm{St} = fA/U$ represents the ratio of the average speed of the filament trailing edge to the oncoming flow speed. It indicates the ratio of the kinetic energy between the filament and the fluid. The fact that St of F_B is much larger than that of F_A suggests F_B extracts much more energy from the flow.

In the following paragraphs, the details of force and energy of the filaments are investigated. We derive a kinematic equation according to the experimental data to estimate the dynamic characteristics of the filaments. The stretch of the filaments is too small to be acquired from experiment videos. Therefore an Euler-Bernoulli beam model is applied to the filaments.

The experimental results show that the undulation of the filaments can be well fitted in terms of a travelling harmonic wave with a spatially varying envelope, which is expressed as

$$y(s, t) = A(s)\sin[2\pi ft + \phi(s)], \tag{1}$$

where s is the length along the filament from the leading edge, t is time, y is the displacement normal to the flow direction, $A(s)$ is the spatial envelope, f is the flapping frequency, and $\phi(s)$ represents the phase along s. The x coordinate can be written as $x(s, t) = \int_0^s \sqrt{1 - (\partial y/\partial s)^2}\,ds$.

Using the extended Hamilton's principle [22,23], the governing differential equation of the beam is given by

$$f_y(s, t) = m_l \frac{\partial^2 y(s, t)}{\partial t^2} + B\frac{\partial^4 y(s, t)}{\partial s^4}, \tag{2}$$

where m_l and B are the linear density and bending stiffness of the filament, respectively. $f_y(s, t)$ is the transverse pressure imposed on the filament. The right hand side of Eq. (2) contains two parts, the effects of inertia and bending stiffness, respectively. Integrating $f_y(s, t)$ along the filament, we can get the transverse hydrodynamic force imposed on the filament, $F_y(t) = \int_0^L f_y(s, t)ds$.

When flapping in the fluid, the filament exchanges energy with the surrounding fluid. The total energy fluctuates around an average energy level. The kinetic energy E_k, elastic potential energy E_p, and the total energy per cycle E, can be expressed as follows, where$T$ is the period.

$$\begin{aligned} E_k(t) &= \frac{1}{2}\int_0^L m_l\left[\left(\frac{\partial x}{\partial t}\right)^2 + \left(\frac{\partial y}{\partial t}\right)^2\right]ds, \\ E_p(t) &= \frac{1}{2}\int_0^L B\frac{(\partial y^2/\partial s^2)^2}{1 - (\partial y/\partial s)^2}\,ds, \\ E &= \frac{1}{T}\int_{t_0}^{t_0+T}[E_k(t) + E_p(t)]dt. \end{aligned} \tag{3}$$

Using the material parameters $m_l = 1.3 \times 10^{-5}$ kg/m, $B = 6.2 \times 10^{-10}$ Pa · m^4 together with the fitted undulation equation, we can calculate the force and energy of the filaments. Figure 4 shows the computation result when $L_b = 20$ mm and $U = 1.9$ m/s. Figure 4(a) is the photo of F_B when its leading edge meets a vortex core. Figure 4(b) shows the distribution of force f_y along F_B at that moment. In Fig. 4(b), the positive value represents the force pointing up. The total force f_y is positive at the leading edge whereas the remaining part of the filament receives a negative force. As is well known, the vortex core is a low pressure region. The distribution of force along the filament matches the arrangement of vortex cores. Integrating the force f_y along F_B, we obtain an downward

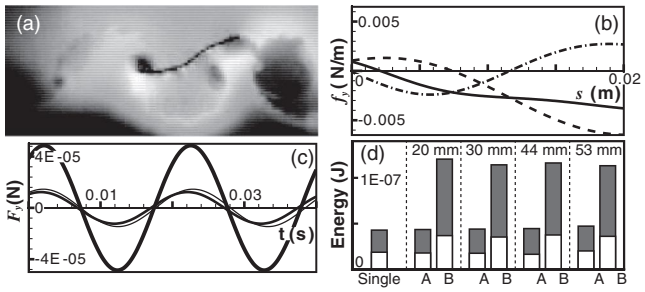

FIG. 4. Force and energy of the filaments ($L_b = 20$ mm, $U = 1.9$ m/s). (a, b) show the force distribution along F_B when it first meets the vortex. The positive value represents the force pointing up. The dash, dash-dot, and solid lines denote the inertia part, the bending stiffness part, and the total force, respectively. (c) shows the comparison of integrated force F_y between filaments: thin, normal and thick lines denote a single filament in a uniform flow, F_A, and F_B in the vortex street, respectively. All the filaments have the same length. (d) shows the energy comparison between a single filament and F_A and F_B with distance $d = 20$, 30, 44 and 53 mm. The gray part is the kinetic energy and the white part is the elastic potential energy.

force -4.28×10^{-5} N and a clockwise moment around the center of the filament 1.39×10^{-7} N · m. Although the leading edge of the filament receives a positive force, the integrated force is still negative, together with a clockwise moment which makes the filament move downwards and rotate around the vortex core instead of ripping into it. The length of the filaments plays an important role. A very short filament compared with the distance of vortex pairs might behave differently from what is mentioned above. We observed, in some experiments, that a downstream filament shorter than 10 mm indeed goes through the vortex cores in one row of the vortex street along the stream while leaving the vortex cores in the other row untouched. This suggests the length is an important factor which makes the filament slalom among the vortex cores.

Figure 4(c) gives a comparison of integrated force among a single filament, F_A and F_B, where $t = 0$ represents the moment when their trailing edges flap passed the equilibrium position upward. All the filaments have the same length. The force imposed on F_A has little difference compared to a single filament of equal length in a uniform flow, but the force on F_B is much larger than that of the other two. This means that during the interaction, the effect on the downstream filament is much more severe than that on the upstream one. Figure 4(d) shows the average energy on the filaments in the same conditions but different downstream distances d. The kinetic and elastic potential energies of F_A keep mostly the same as those of a single filament, regardless of the distance changing between F_A and F_B. However, the energy of F_B increased a lot for all distances d, indicating clearly that F_B certainly extracts energy from the vortex street.

It is known that energy exchange should occur between the kinetic and elastic potential energies of the filament, and between filaments and the fluid. In other words, when a filament is located in a flow field, the filament acquires energy from the surrounding fluid, restores the energy in the forms of kinetic and elastic potential energies, then transfers them along the filament and finally releases the energy to the fluid. The kinetic and elastic potential energies fluctuate and become balanced during this process. For a single filament in a uniform flow and F_A in the serial interaction, a balance between kinetic and elastic potential energies occurs [see Fig. 4(d)]. But when calculating the energy budget of F_B, we find the total energy increases greatly, indicating clearly that F_B extracts energy from the vortex street. In addition, the increased kinetic energy is much larger than the elastic potential energy, indicating that the extracted energy is used to enhance the kinetic energy of filament. The inertia of the filament plays an important role in this phenomenon, in that it allows the filament to have a delayed response to the pressure imposed on it.

The observation of the filaments' passive oscillation and a live fish swimming in the Kármán vortex street is similar. Both of them slalom among the vortex cores. In the passive oscillation of filaments, the filaments are driven by the pressure produced by the vortices and flap at the same frequency as the vortex street. Lifeless filaments do not actively take advantage of the wake. This is different from active swimming. Live animals know how to deal with the wake. They effectively utilize the passive deformations of their flexible bodies in a flow field and extract more energy from the wake to help them reduce their own energy expenditure; thus, only little muscle action is needed in swimming in the vortex street. Nevertheless, the similarity between the filament flapping and fish swimming is not superficial [18]. The study of passive oscillation is still essential in understanding the mechanisms in both swimming and flight movements in nature.

This work was supported by the NSFC (No. 10332040) and CAS (No. KJCX2-YW-L05).

*xzyin@ustc.edu.cn

[1] D. Cushing and F. Harden-Jones, Nature (London) **218**, 918 (1968).
[2] D. Weihs, Nature (London) **241**, 290 (1973).
[3] B. Partridge and T. Pitcher, Nature (London) **279**, 418 (1979).
[4] J. Herskin and J. Steffensen, J. Fish Biol. **53**, 366 (1998).
[5] J. C. Liao, D. N. Beal, G. V. Lauder, and M. S. Triantafyllou, Science **302**, 1566 (2003).
[6] G. Dong and X. Lu, Phys. Fluids **19**, 057107 (2007).
[7] G. Lauder, E. Anderson, J. Tangorra, and P. Madden, J. Exp. Biol. **210**, 2767 (2007).
[8] I. Akhtar, R. Mittal, G. Lauder, and E. Drucker, Theor. Comput. Fluid Dyn. **21**, 155 (2007).
[9] D. N. Beal, F. S. Hover, M. S. Triantafyllou, J. C. Liao, and G. V. Lauder, J. Fluid Mech. **549**, 385 (2006).
[10] J. Liao, Phil. Trans. R. Soc. B **362**, 1973 (2007).
[11] J. Zhang, S. Childress, A. Libchaber, and M. Shelley, Nature (London) **408**, 835 (2000).
[12] Y. Couder, J. M. Chomaz, and M. Rabaud, Physica (Amsterdam) **37D**, 384 (1989).
[13] M. Gharib and P. Derango, Physica (Amsterdam) **37D**, 406 (1989).
[14] M. A. Rutgers, Rev. Sci. Instrum. **72**, 3025 (2001).
[15] J. M. Chomaz, J. Fluid Mech. **442**, 387 (2001).
[16] S. Alben, M. Shelley, and J. Zhang, Nature (London) **420**, 479 (2002).
[17] G. Huber, Nature (London) **408**, 777 (2000).
[18] U. Muller, Science **302**, 1511 (2003).
[19] L.-B. Jia, F. Li, X.-Z. Yin, and X.-Y. Yin, J. Fluid Mech. **581**, 199 (2007).
[20] See EPAPS Document No. E-PRLTAO-100-016824 for videos of the filaments' passive oscillations. For more information on EPAPS, see http://www.aip.org/pubservs/epaps.html.
[21] C. Wu, Y. Xie, and J. Wu, Acta Mechanica Sinica **19**, 476 (2003).
[22] K. Behdinan, M. C. Stylianou, and B. Tabarrok, J. Sound Vib. **208**, 517 (1997).
[23] B. S. H. Connell and D. K. P. Yue, J. Fluid Mech. **581**, 33 (2007).